Langmuir

ARTICLE

pubs.acs.org/Langmuir

Symmetric pH-Dependent Swelling and Antibacterial Properties of Chitosan Brushes

Hyun-Su Lee,[†,‡,§] David M. Eckmann,[†,‡] Daeyeon Lee,[∥] Noreen J. Hickok,[⊥] and Russell J. Composto*[,†,§]

[†]Institute of Medicine and Engineering, [‡]Department of Anesthesiology and Critical Care, [§]Department of Materials Science and Engineering, and [∥]Department of Chemical and Biomolecular Engineering, University of Pennsylvania, Philadelphia, Pennsylvania 19104, United States

[⊥]Department of Orthopaedic Surgery and Biochemistry & Molecular Biology, Thomas Jefferson University, Philadelphia, Pennsylvania 19107, United States

Supporting Information

ABSTRACT: Charged polymer brushes grafted to surfaces are of great interest for antibacterial, biosensor, nanofluidic, and drug delivery applications. In this paper, chitosans with quaternary ammonium salts, CH-Q, were immobilized on silicon oxide and characterized by in situ quartz-crystal microbalance with dissipation, QCM-D, and in situ spectroscopic ellipsometry, SE. Both methods showed that the hydrated film exhibited a minimum thickness of ∼40 nm near pH 5 that increased strongly (up to ∼80 nm) at lower and higher pH. This symmetric swelling is surprising because CH-Q is a cationic polymer. The CH-Q grafted layer was stable for pH values from 3 to 8 and exhibited rapid, reversible swelling and contraction upon varying pH. The CH-Q layer also reduced *S. aureus* colonization by a factor of ∼30× compared to bare silicon oxide and an amine terminated silane grafted to silicon oxide. This antibacterial characteristic of CH-Q is attributed to the quaternary ammonium salts and the flexible polymer brush.

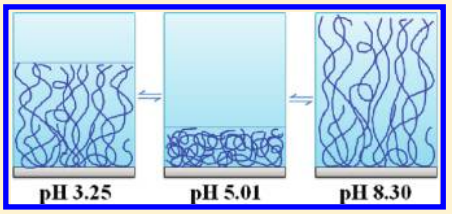

I. INTRODUCTION

Polymer brushes impart surfaces with a wide range of properties including biocompatibility and bacterial resistance. These brushes can be made by grafting synthetic or natural polymers to surfaces.[1−5] In the latter case, chitosan brushes are particularly attractive to explore because chitosan is pH responsive, swelling strongly, and has many potential applications. Recently chitosan has found use in medical and pharmaceutical applications such as drug delivery, wound dressing materials, tissue scaffolds, and antimicrobial coating.[6−9] Chitosan is a random-copolymer of D-glucosamine (GlcN) and *N*-acetyl-D-glucosamine (GlcNAc) linked by β-(1,4) glycosidic bonds. Because the GlcN residue contains a primary amine, the chemical and physical properties of chitosan can be tuned by varying the percentage of GlcN, the degree of deacetylation (DDA). For example, at low pH, chitosan is a water-soluble cationic polyelectrolyte due to its protonated amines; at higher pH (above ∼6.5), chitosan is uncharged and becomes insoluble in water.[10,11]

Although its bulk properties depend on pH (<∼6) and counteranion size,[12−15] chitosan has not been fully utilized as a biomaterial coating because of its limited solubility near physiological conditions (pH ∼ 7). Toward that end, chitosan can become water-soluble at higher pH (above ∼6.5) when it is modified with quaternary ammonium salts, CH-Q,[16] because the quaternary ammonium cation remains positively charged across a wide range of pH. Whereas its bulk and particle properties are well-known, chitosan grafted to surfaces (i.e., polymer brush) has received limited attention. In one study, chitosan was grafted to a poly(ethylene terephthalate) (PET) substrate whose surface was pretreated by surface-initiated radical polymerization of acrylic acid. Grafting was achieved by coupling the amine group of chitosan to the carboxyl acid on the surface, and attenuated total reflection Fourier transform IR (ATR-FTIR) and electron spectroscopy for chemical analysis (ESCA) were used to characterize the surfaces. Relative to PET alone, the modified surfaces were found to inhibit bacterial growth.[17] Chitosan films have also been prepared by an electrodeposition method where a high pH adjacent to the cathode resulted in the deposition of insoluble chitosan.[10,11]

Polymer brushes are well-known to respond to changes in temperature, solvent, pH, and ionic strength.[18−26] For example, neutral polymer brushes of poly(*N*-isopropylacrylamide) respond to changes in temperature due to a phase transition in water near 32 °C, whereas polystyrene brushes respond by swelling or collapsing in good and poor solvents, respectively.[19,20] Polyelectrolyte polymer brushes such as anionic poly(acrylic acid) respond to changes in ionic strength and pH by undergoing large conformational changes, whereas cationic brushes of [2-(methacryloyloxy)ethyl]trimethylammonium chloride (METAC) respond to changes in ionic strength and electrolyte environment (e.g., NaCl and $MgSO_4$).[21−24] Block copolymer brushes and mixtures of homopolymer brushes having selective solvent affinities for each block or homopolymer, respectively, have been studied.[25,26]

Received: July 9, 2011
Revised: September 2, 2011
Published: September 06, 2011

Recently, polyelectrolyte multilayers were shown to strongly swell in a reversible manner upon exposure to stimuli such as pH and ionic strength.[27,28] These multilayers have been widely investigated because their tunable swelling properties can be used to create stimuli-responsive surfaces and interfaces for controlling drug release and modulating cell adhesion. Unfortunately, some applications are limited by the stability of the electrostatic interactions that hold the polycation and polyanion layer together. As noted in this paper, chemically grafted chitosan brushes are stable and exhibit reversible, symmetric swelling upon varying pH.

Positively charged macromolecules such as proteins (protegrin, magainin, indolicidin, and other antimicrobial peptides)[29] and synthetic polymers modified with guanidinium salts,[30] phosphonium salts,[31] and quaternary ammonium salts[31−38] have been of interest for antimicrobial applications. Grafted to surfaces, these cationic polymer layers are bactericidal because they decrease bacterial ATP levels and metabolic activity.[39] Quaternary ammonium salts have been chemically attached to synthetic polymers and biopolymers as a means to create coatings with antibacterial properties.[31−38]

In this study, chitosan with quaternary ammonium salts, CH-Q, is grafted to the epoxide derivatized silicon oxide surfaces to create an antibacterial surface. Zeta-potential measurements show that the CH-Q surface remains highly positively charged for pH values ranging from 2.97 to 8.21, as expected for a cationic polymer. The pH-dependent swelling behavior of this CH-Q grafted layer is investigated using complementary in situ characterization methods, namely, quartz crystal microbalance with dissipation (QCM-D)[20,23,40−42] and spectroscopic ellipsometry (SE).[27,28,43,44] In situ QCM-D and in situ SE studies show that immobilized CH-Q is chemically stable over a wide range of pH values and exhibits reversible swelling and contraction that can be tuned by varying the pH of the solution. The CH-Q layer has minimum thickness, ∼30 nm, near pH 5.01. Although the layer thickness is a minimum near pH 5.01, the water concentration in the swollen CH-Q is relatively high, 78%. At higher and lower values of pH, the CH-Q layer thickness increases significantly, swelling up to ∼3× the thickness at pH 5.01. Because the CH-Q layer is a cationic polymer, the symmetric swelling behavior around pH 5.0 is unexpected. The CH-Q thicknesses and water concentrations determined by in situ SE and in situ QCM-D are in excellent agreement with each other. In an initial test of antibacterial efficacy, CH-Q surfaces are exposed to *Staphylococcal aureus* (*S. aureus*, ATCC 35556) and found to reduce *S. aureus* colonization by a factor of ∼30×, relative to silicon oxide and amine terminated silicon oxide surfaces.

II. EXPERIMENTAL SECTION

Materials. Chitosan Chitoclear Cg-10 (M_w = 60 kDa and degree of deacetylation = 87%) was received from Primex ehf., Iceland. N-Type, (100) oriented silicon wafers (CZ silicon, dopant; Ph, 20−30 Ω resistivity) were purchased from Silicon Quest International. QCM sensor crystals, an AT-cut piezoelectric quartz crystal (14 mm in diameter and 0.3 mm thickness) coated with a 50 nm thick layer of silicon dioxide, were purchased from Biolin Scientific, Inc. 3-Glycidoxypropyl-trimethoxysilane (GPTMS, ≥98%), 3-aminopropyltriethoxysilane (APTES, ≥98%), 80 wt % aqueous solution of [(2-(acryloyloxy)ethyl]trimethylammonium chloride (AETMAC), 5 M sodium chloride solution, tris(hydroxylmethyl)aminomethane (TRIS, ≥99.9%), and anhydrous toluene (99.8%) were purchased from the Aldrich Chemical Co. Ultrapure water (Millipore Direct-Q, 18 MΩ cm resistivity) was used for the preparation of all solutions. *S. aureus* (ATCC 35556) was obtained from PML Microbiologicals, Wilsonville, OR. Brain heart infusion (BHI), BBL trypticase soy broth (TSB), Bacto agar, and phosphate buffered saline tablets (PBS) were purchased from Fisher Scientific.

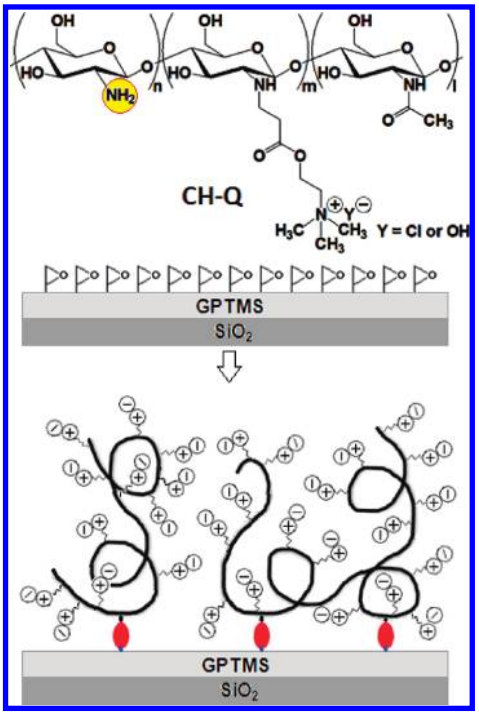

Figure 1. (top) The chemical structure of water-soluble chitosan modified with quaternary ammonium salts (CH-Q). CH-Q is "grafted to" epoxide-derivatized silicon oxide surfaces via the primary amine functional groups of CH-Q (yellow circle). (bottom) Red ovals represent the covalent grafting of the primary amine of CH-Q with the epoxide group. The quaternary ammonium cation and counteranions (Y^-) are denoted as plus and minus, respectively.

Polymer Synthesis and Characterization. Chitosan with quaternary ammonium salts, CH-Q (see Figure 1), was prepared by Michael reaction of chitosan with acryl reagent (AETMAC) in water and characterized by using ^{1}H NMR experiments according to the literature.[16] ^{1}H NMR spectra was obtained using a Bruker 360 MHz spectrometer in the department of chemistry at the University of Pennsylvania. The degree of substitution of the chitosan derivative, DS, was calculated by using ^{1}H NMR according to the literature.[16] For degree of deacetylation (87%, l = 0.13), 51% of monomers are functionalized with quaternary ammonium salts (DS = m = 0.51). Data for CH-Q (DS = 0.51): ^{1}H NMR (360 MHz, 0.5 M DCl in D_2O, ppm) 2.06 (s, 0.39 H, $NHCOCH_3$), 2.91 (s, 1.01 H, $-CH_2-CO_2-$), 3.13 (s, NMe_3), 3.28 (s, *H-2* of GlcN), 3.31 (s, *H-2* of N-alkylated GlcN), 3.6−4.1 (m, $N-CH_2-$ and $-CH_2-CH_2-$ of N-alkyl group, *H-2* of GlcNAc, *H-3,4,5,6* of GlcN and GlcNAc), 4.61 (br, *H-1* of GlcNAc), 5.04 (br, *H-1* of N-alkylated GlcN).

Surface Preparation and Characterization. Silicon wafers (35 mm × 15 mm for zeta potential and SE measurements, 30 mm × 25 mm for antibacterial experiments) and SiO_2-coated QCM sensor crystals were cleaned by immersion in piranha solution (3:1 (v:v) H_2SO_4/30% H_2O_2 (Fisher Scientific)), rinsed with ultrapure water (Millipore Direct-Q, 18 MΩ cm resistivity), dried with N_2, and exposed to UV−ozone to produce an homogeneous hydroxylated surface and to remove impurities. Each silane deposition on silicon oxide surfaces was performed by immersion of the wafers and crystals into 10% (v/v) 3-glycidoxypropyltrimethoxysilane (GPTMS) and 5% (v/v) 3-aminopropyltriethoxysilane (APTES) in anhydrous toluene at 80 °C for 12 h under N_2, respectively.

The deposited samples were sonicated in toluene to remove physically absorbed GPTMS and impurities on the surface.

To immobilize CH-Q on an epoxide-derivatized (GPTMS) silicon oxide surface, the GPTMS surface was immersed in 2 wt % aqueous solution (10 mL) of CH-Q (pH 7.8), water was evaporated slowly, and the CH-Q film was made by direct contact with the GPTMS surface at 60 °C, overnight (~12 h). The surface was rinsed with the ultrapure water to remove physically adsorbed CH-Q and other impurities on the surface. For the surface characterization, the thicknesses of dry substrate on the surface were measured by using an alpha-SE ellipsometer (J.A. Woollam Co., Inc., Lincoln, NE) equipped with a wavelength range from 380 to 900 nm (70° angle of incidence). Contact angles were measured by using a 1 μL sessile drop method.

Flat Surface Zeta Potential Measurement. The zeta-potential of flat surface samples was measured via a DelsaNano-C (Beckmann Coulter) instrument by using the flat surface cell. The electrophoretic mobility of probe particles between a flat surface sample and cell surface was measured by using electrophoretic light scattering. The zeta potential in volts (ζ) was calculated by the Smoluchowski equation:

$$\zeta = k\frac{\pi\eta}{\varepsilon}U$$

where η is the viscosity of the solution at 25 °C, ε is the dielectric constant of the solution at 25 °C, and U is the electrophoretic mobility of probe particles. Each measurement was the average of 70 individual measurements performed at various positions (10 measurements each in 7 positions). All measurements were done in at least triplicate. Solution pH was measured with a dual pH/conductivity meter (Dever Instrument Co. USA). Solutions of 10^{-3} M TRIS and 10^{-3} M solutions with probe particles (140 μL, base frequency ~ 120 Hz) were prepared. Solution pH was regulated by titration with 1 M NaOH and 1 M HCl.

In Situ QCM-D Measurement. The QCM-D measurement is based on the resonance frequency change of a vibrating quartz crystal, a piezoelectric material, when mass is deposited on it. The deposited mass, Δm, has a relationship with the frequency change, Δf, according to the Sauerbrey equation,[20,23,40−42]

$$\Delta m = -C\frac{\Delta f_n}{n}$$

where C is the mass sensitivity constant (C = 17.7 ng·cm^{-2}·Hz^{1-} for an AT-cut, 5 MHz crystal) and n is the vibrational mode number (n = 1, 3, 5, ...). In addition, the dissipation change, ΔD_n, the loss of energy stored in a vibration cycle, indicates the physical characteristics of the deposited layer such as viscosity, elasticity, and so on. If ΔD_n is less than 2.0×10^{-6} and the plots of $\Delta f_n/n$ under several modes are superimposed, the layer is an elastic film. The physical properties (mass and thickness) of the elastic layer can be calculated using the Sauerbrey equation.[40,41] On the contrary, if ΔD_n is more than 2.0×10^{-6} and the plots of $\Delta f_n/n$ are not superimposed, the layer is viscoelastic. The physical properties (thickness, shear modulus, and viscosity) of the viscoelastic layer can be estimated fitting between the QCM-D experimental data ($\Delta f_n/n$ (n = 1, 3, 5, ...) and ΔD_n) and a Voigt-based viscoelastic model incorporated in Q-Sense software Q-Tools.[20,23,42]

An E4 QCM instrument (Q-Sense Inc., Gothenburg, Sweden) was used to monitor the pH-dependent conformational changes of immobilized CH-Q layer on SiO_2-coated QCM sensor crystals. Solution pH was measured with a dual pH/conductivity meter (Dever Instrument Co. USA). Solution pH was adjusted by titration with 1 M NaOH and 1 M HCl. All different pH solutions were degassed by sonication. The liquid medium was pumped by peristaltic pump at a rate of 20 μL/min through a flow cell with the sensor crystal. The temperature of the system was controlled to 21 °C.

As a control, we first monitored $\Delta f_n/n$ (n = 3, 5, 7) and ΔD_n for the bare SiO_2-coated QCM sensor because changes in the solution composition can induce changes in frequency and dissipation due to variations in viscosity and elasticity. When solutions with pH values of 3.25, 5.01, 7.17, and 8.30 were successively introduced, $\Delta f_n/n$ was found to be constant within ±0.5 Hz. ΔD_n was also invariant with solution composition. This shows that upon switching between the different pH solutions, the observed changes in frequency and dissipation for the grafted CH-Q layer are attributed to changes in the conformation of the CH-Q layer as it swells or contracts.

In Situ SE Measurement. According to the literature,[27,28,43,44] a homemade liquid cell was used to measure the swelling of the CH-Q layer on silicon wafer in different pH solutions (the same pH solutions used for QCM-D). In situ SE measurements were carried out using an Alpha-SE ellipsometer. The liquid cell accuracy was verified by measurements of spin-coated polystyrene films according to the literature.[27,28] The error in the thickness measurement was determined to be within ±3%.

Swelling Studies. To understand the pH dependent swelling behavior, the percent swelling was calculated from the dry thickness and the pH-dependent swollen thicknesses determined by in situ SE and in situ QCM-D according to the literature.[28] The percentage swelling of the CH-Q layer is defined as

$$\%\ \text{swelling} = \frac{T_{\text{insitu}} - T_{\text{dry layer}}}{T_{\text{dry layer}}} \times 100$$

where $T_{\text{dry layer}}$ is the dry thickness of the CH-Q layer and $T_{\text{in situ}}$ is the CH-Q thickness obtained from in situ methods.

Bacterial Culture and Antibacterial Test. Sterilized APTES, silicon oxide, and CH-Q surfaces were used to determine the effects of surface treatment on bacterial adhesion. APTES surface was used as a reference since the surface is well-known as a favorable surface for bacteria growth.[38] *S. aureus* was cultured in brain heart infusion (BHI) broth, 175 rpm, 37 °C, 12−16 h (overnight culture) and diluted to ~1×10^4 cfu/mL using a 0.5 McFarland standard, a turbidity standard which is equivalent to 10^7−10^8 cfu/mL of *S. aureus* (PML Microbiologicals, Wilsonville, OR). APTES, silicon oxide, and CH-Q surfaces were immersed in the diluted bacterial solution (pH 7.3) at 37 °C for 6 h with shaking at 100 rpm, immersed in sterilized PBS solution at 37 °C for 20 min with shaking at 100 rpm, air-dried (2 min), and incubated under a thin film of TSB agar (3% agar), 37 °C, 12−16 h (overnight). Surface colonization was digitally recorded; numbers of colonies were counted and colony count normalized to an area of 1 × 4/3 cm. All experiments were performed at least three times, with photographs of the experiments analyzed to determine average (±standard deviation) colony counts per unit area.

III. RESULTS AND DISCUSSION

Immobilization of Chitosan with Quaternary Ammonium Salt, CH-Q, on Silicon Oxide Surface. CH-Q was prepared by a Michael reaction of chitosan with an acryl reagent (AETMAC) in aqueous solution. Using ^{1}H NMR, the monomer fractions of D-glucosamine (GlcN), *N*-alkylated D-glucosamine with quaternary ammonium salts (GlcN-Q), and *N*-acetyl-D-glucosamine (GlcNAc) are n = 0.25, m = 0.51, and l = 0.13, respectively (Figure 1). These monomer fractions are in good agreement with the values from the literature.[16] The solubility of CH-Q was determined in hydrogen chloride or sodium hydroxide solution across the pH range 3−9. One of the most interesting observations is that "bulk" CH-Q is soluble below pH 5 and above pH 6, but for pH values between pH 5 and 6 CH-Q forms aggregates in solution. In the following experiments, we have designed grafted CH-Q on surfaces to take advantage of the reversibility of CH-Q swelling and contraction during exposure to environments of varying pH.

The well-known epoxide-amine reaction is used to immobilize CH-Q on silicon oxide surfaces, including glass microscope slides, hydroxylated silicon wafers, and silicon oxide coated QCM sensors (Figure 1). First, silicon oxide surfaces are modified with epoxide functional groups by reacting trimethoxy silane groups of 3-glycidoxy-propyltrimethoxysilane (GPTMS) and hydroxyl groups on silicon oxide surfaces. The thickness values measured by SE and water contact angles of silicon oxide and GPTMS derivatized layers (Supporting Information Table S-1) are in reasonable agreement with literature values.[45,46] To graft CH-Q, the primary amine functional groups from the GlcN units react with the epoxide groups on the surface, resulting in stable covalent bonds (Figure 1). The CH-Q grafted layer has a dry thickness of 6.0 nm, and the water contact angle is ~0 (Supporting Information Table S-1). These results suggest that CH-Q is chemically grafted to the GPTMS derivatized surface and the CH-Q grafted layer is hydrophilic.

The interaction between bacteria and a surface will depend on the sign and magnitude of the surface charge density. The surface charge of silicon oxide and CH-Q grafted surfaces was characterized by measuring the zeta potential at pH values between 2.97 and 8.21. The zeta potential of silicon oxide is -9 ± 4 mV at pH 2.97, decreases strongly to -43 ± 3 mV at pH 3.70, and then decreases weakly to -74 ± 1 mV as pH approaches 8.21 (Supporting Information Figure S-1). This behavior is consistent with literature reports.[47−49] Upon grafting CH-Q via GPTMS to this oxide, the negatively charged silicon oxide becomes positively charged due to the addition of quaternary ammonium and protonated amine cations (Supporting Information Figure S-1). The conversion from negatively to highly positively charged surfaces across the pH range provides further evidence that CH-Q is grafted to the epoxide derivatized silicon oxide surface. The zeta potential of the CH-Q immobilized surface at pH 8.19 is $+39 \pm 7$ mV. As pH is reduced to 7.30, the zeta potential increases to $+49 \pm 1$ mV and then remains relatively constant as pH is lowered further (i.e., $+55 \pm 2$ mV in pH 5.55, $+51 \pm 3$ mV in pH 4.14, and $+50 \pm 5$ mV in pH 3.01). This pH dependence can be explained by examining the charge on the ammonium groups. For all values of pH, the positive charge contributed by stable quaternary ammonium groups is fixed. At a more acidic pH, the CH-Q layer exhibits a higher positive charge because primary and secondary amines of CH-Q become fully protonated; once protonated, a further reduction in pH does not alter the surface charge. However, at higher pH (pH 8.19), the CH-Q layer is less positively charged as the pH approaches the pK_a of the primary and secondary ammonium groups (~11).

In Situ Studies Using QCM-D and SE. CH-Q molecules in solution form aggregates between pH 5 and 6, but are soluble for pH values below 5 and above 6. To take advantage of this change in solubility, CH-Q was grafted to the epoxide derivatized silicon oxide and observed in situ as a function of pH using QCM-D measurement. Figure 2a shows the QCM-D results for the immobilized CH-Q layer on the SiO_2 coated sensor upon switching the pH of the solution. For the three modes ($n = 3, 5, 7$), $\Delta f_n/n$ of the CH-Q layer exposed to pH 5.01 solution superimposes and ΔD_n exhibits its lowest value, $\sim 4 \times 10^{-6}$. This result suggests that the CH-Q layer exhibits elastic behavior at pH 5.01. Upon decreasing the pH from 5.01 to 3.25 (arrow 1), $\Delta f_n/n$ ($n = 3, 5, 7$) decreases and the curves no longer superimpose, whereas ΔD_n increases. This change means that an increase in water content within the layer at the reduced pH results in a more swollen and viscous CH-Q layer. Upon increasing the pH from 3.25 back to pH 5.01 (arrow 2), $\Delta f_n/n$ ($n = 3, 5, 7$) and ΔD_n return to their original values. This means that during the pH exposure the mass of CH-Q grafted layer did not change and the CH-Q layer is chemically stable. The increase and superposition of $\Delta f_n/n$ ($n = 3, 5, 7$) and the decrease of ΔD_n mean that a decrease in water content of the layer leads to the original elastic CH-Q layer. For pH > 5.01, the extent of swelling varied with pH. Upon increasing the pH from 5.01 to 7.17 (arrow 3), $\Delta f_n/n$ ($n = 3, 5, 7$) and ΔD_n weakly decrease and increase, respectively. In contrast, upon increasing the pH from 5.01 to 8.30 (arrow 5), $\Delta f_n/n$ ($n = 3, 5, 7$) and ΔD_n strongly decrease and increase, respectively. Thus, at pH 8.30, more water penetrates into the CH-Q layer, resulting in more swollen and viscous layer than at pH 7.17. After every subsequent change in pH (arrows 3, 4, 5, and 6), similar reversible behavior is observed when the solution pH returns to 5.01. These studies demonstrate that the immobilized CH-Q layer is chemically stable over a wide range of pH values and exhibits reversible swelling and contraction that can be tuned by varying the pH of the solution. At values above and below pH 5.01, an increase in water content within the layer results in a more swollen and viscous CH-Q layer. In contrast, at pH 5.01, the CH-Q layer expels water and contracts. For end grafted polyanionic brushes, self-consistent mean field (SCF) theory has shown that the outer brush contains a higher concentration of water than the region adjacent to the substrate.[50] Because QCM-D only responds to the average film properties, applying SCF theory to our system would provide further insight into the volume fraction profile of water within the brush.

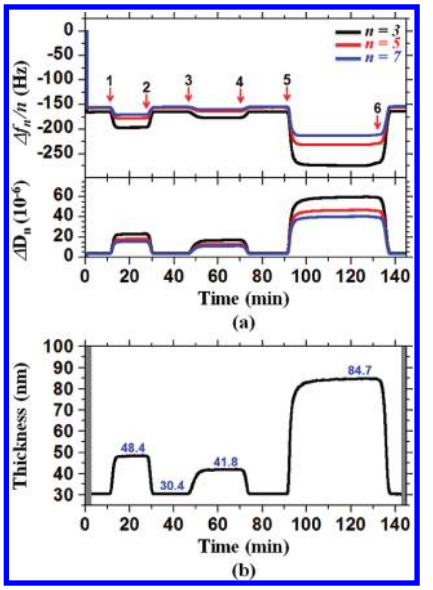

Figure 2. (a) Traces of $\Delta f_n/n$ ($n = 3, 5, 7$) and ΔD_n versus time as a function of sequential changes in solution pH. Arrows 1, 2, 3, 4, 5, and 6 represent the change from pH 5.01 to 3.25, pH 3.25 to 5.01, pH 5.01 to 7.17, pH 7.17 to 5.01, pH 5.01 to 8.30, and pH 8.30 to 5.01, respectively. (b) Thickness versus time determined from the best fit of the experimental data (c.f. Supporting Information Figure S-2) with the viscoelastic model.[51]

Physical properties of the layer such as thickness, shear modulus, and viscosity can be calculated based on the fit between the Voigt based-viscoelastic model[51] and the QCM-D experimental data.[20,41,42] The CH-Q layer thicknesses obtained from the fit (Supporting Information Figure S-2) between the viscoelastic model and the experimental data ($\Delta f_n/n$ ($n = 3, 5$) and ΔD_n) are plotted versus

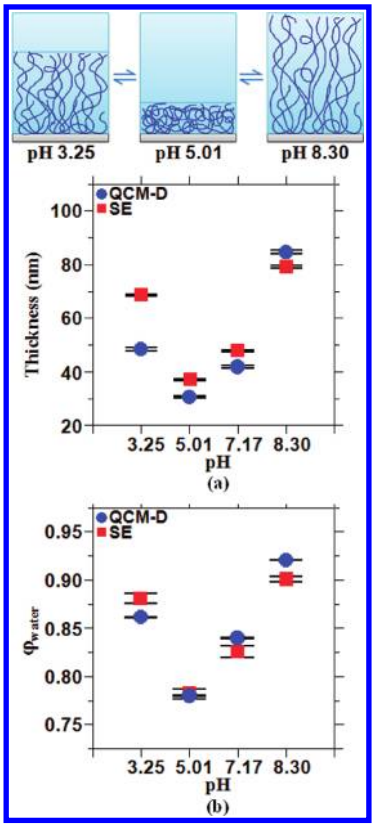

Figure 3. (a) Thickness versus pH from in situ QCM-D and in situ SE. (b) Infused water fractions in CH-Q layer in each pH solution from in situ QCM-D and in situ SE.

time (as a function of pH) in Figure 2b. At pH 5.01, the thickness of the CH-Q layer is 30.4 ± 0.21 nm. Upon decreasing the pH from 5.01 to 3.25 (arrow 1), the layer thickness increases to 48.4 ± 0.69 nm. Upon increasing pH from 3.25 back to pH 5.01 (arrow 2), the layer thickness returns to the original value of 30.4 ± 0.21 nm. After each change in pH (arrows 3, 4, 5, and 6), the same thickness is recovered as expected for reversible behavior (arrow 1 and 2). At pH 7.17, the CH-Q layer is swollen and the thickness is 41.8 ± 0.45 nm. When the pH increases from 5.01 to 8.30 (arrow 5), the CH-Q layer is most swollen with a thickness of 84.7 ± 0.67 nm. These studies demonstrate that the immobilized CH-Q layer can swell by nearly 3× its original thickness in a reversible manner. In addition to thickness, the model provides values of the shear modulus of the CH-Q layer at each pH. This data is given in Figure S-2 in the Supporting Information.

To complement the QCM-D studies and further understand the interplay between swelling behavior of CH-Q layer and pH, the thickness and *refractive index* of the CH-Q layer were measured using in situ spectroscopic ellipsometry (SE) at pH values 3.25, 5.01, 7.17, and 8.30. By in situ SE, at pH 5.01, the CH-Q thickness exhibits a minimum value, 36.9 ± 0.3 nm, similar to that measured with in situ QCM-D (Figure 3a). As pH decreases from 5.01 to 3.25, the CH-Q thickness markedly increases to 68.6 ± 0.4 nm. Similarly, as pH increases from 5.01 to 7.17, the CH-Q thickness increases to 47.8 ± 0.3 nm. Upon further increasing pH to 8.30, the CH-Q layer thickness increases to its largest value, 79.2 ± 0.5 nm, again similar to that measured with in situ QCM-D. After each SE measurement (pH 3.25, 7.17, and 8.30), the material at pH 5.01 returns to its original thickness. This reversible swelling and contraction measured with in situ SE is consistent with the reversible behavior observed using QCM-D (cf. Figure 2). This quantitative agreement suggests that similar thicknesses are measured for grafted layers both under quiescent conditions of SE experiments as well as flow conditions in the QCM-D experiments. Importantly, the effect of pH on the grafted CH-Q layer is consistent with the solubility behavior previously noted for CH-Q.

To determine if thickness values, 40−80 nm, measured by QCM-D and SE are physically reasonable, the dimensions of CH-Q are estimated from measurements of chitosan under acidic conditions.[7,52,53] For a radius of gyration, R_g (nm) = 0.0064 $M_w^{0.55}$, R_g of chitosan with M_w = 60 kDa is 27.2 nm.[5] The large coil size of chitosan is attributed to its stiff wormlike chain characteristics as noted by a persistence length of ∼12 nm.[52,53] For chitosan with 87% deacetylation, the contour length, l_c, is 186 nm. Thus, the measured thickness values are physically reasonable. For h = 40 nm, these values indicate that CH-Q is grafted by two to three covalent bonds to the surface. Note that this calculation does not include contributions from the quaternary ammonium cation and polydispersity.

The water content of the swollen CH-Q layer at each pH (3.25, 5.01, 7.17, and 8.30) can be calculated from the refractive index and thickness determined by in situ SE and in situ QCM-D, respectively. The volume fraction of water, φ_{water}, in the CH-Q layer can be estimated by the rule of mixtures equation:

$$\varphi_{water} = \frac{n - n_{CH}}{n_{water} - n_{CH}}$$

where n_{CH} and n_{water} are the refractive indexes of chitosan and pure water at 633 nm (1.500 and 1.331, respectively[54,55]) and n is the refractive index of the hydrated CH-Q layer at 633 nm. The volume fraction of water in the CH-Q layer can also be estimated from the volume of dry CH-Q layer and total volume of the hydrated CH-Q layer determined from QCM-D. Figure 3b shows the volume fractions of water in the CH-Q layer at each pH determined from in situ SE and in situ QCM-D. At pH 5.01, the water volume fractions exhibit minimum values of 0.781 ± 0.006 (n = 1.368 ± 0.001) and 0.780 ± 0.002, respectively. This means that, at pH 5.01, the CH-Q layer is 78% water and 12% CH-Q. According to QCM-D, the CH-Q layer has its lowest value of the damping component at this pH and correspondingly its mechanical properties are dominated by elasticity. As pH decreases from 5.01 to 3.25, the water fractions increase to 0.882 ± 0.005 (n = 1.351 ± 0.001) and 0.861 ± 0.001, respectively. As pH increases from 5.01 to 7.17, the water fractions also increase to 0.825 ± 0.006 (n = 1.361 ± 0.001) and 0.840 ± 0.001, respectively. At pH 8.30, the CH-Q layer absorbs the greatest amount of water, 0.901 ± 0.003 (n = 1.348 ± 0.001) and 0.921 ± 0.001, respectively. Upon comparison with the QCM-D results (Figure 2), the CH-Q layer has its highest damping component at pH 8.30 and correspondingly the swollen CH-Q layer is dominated by viscous behavior. These studies support the previous observations of pH dependent swelling of CH-Q. Note that the water fractions in the CH-Q layer determined by in situ SE and in situ QCM-D are in excellent agreement. Using both SE and QCM-D, new insight is gained about CH-Q film behavior showing that, even at pH 5.01, where film thickness is at a minimum, CH-Q contains a high concentration of water (78%). Furthermore, relatively small changes in water content (e.g., 78−90%) appear to be sufficient to trigger an order of magnitude reduction in the shear modulus of CH-Q.

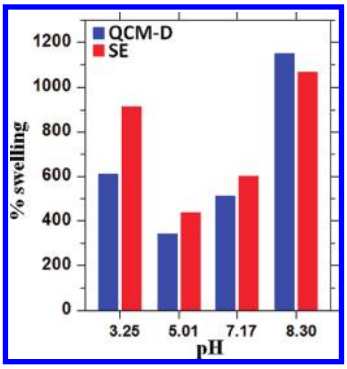

Figure 4. Percent swelling of grafted CH-Q determined by in situ QCM-D and in situ SE at different pH conditions.

To understand the pH dependent swelling behavior, the percent swelling was determined from the dry thickness and the pH-dependent swollen thicknesses determined by in situ QCM-D and in situ SE (Figure 4). At pH 5.01, the percent swelling from the dry CH-Q layer in aqueous solution is 350% and 450%, respectively. According to QCM-D, although the CH-Q layer exhibits mainly elastic behavior at pH 5.01, the layer is highly swollen with water. As pH decreases from 5.01 to 3.25, the swelling increases to 620% and 920%, respectively. Upon increasing pH from 5.01 to 7.17, the swelling increases to 520% and 610%, respectively. At pH 8.30, the CH-Q layer is most swollen and the swelling increases to 1160% and 1080%, respectively. After each measurement of the swollen state, the CH-Q film thickness returned to its original value after drying. These studies demonstrate that the CH-Q layer is highly swollen for pH values from 3 to 8.3, swelling is a minimum at pH 5.01, and swelling is reversible. The thickness of polyelectrolyte brushes has been shown to depend on pH.[5,21] For example, upon increasing the pH from 2 to 10, the thickness of poly(acrylic acid) brushes increases from 16 to 26 nm. A general trend for polyanionic brushes is that chains collapse as pH decreases. Correspondingly, polycationic brushes swell as pH decreases. Whereas polyanionic and polycationic brushes exhibit monotonic behavior as pH is reduced, CH-Q brushes display a symmetric swelling behavior with a minimum thickness near pH 5.

These observations lead to the hypothesis that the swelling behavior of grafted CH-Q results from intra- and intermolecular electrostatic repulsion due to quaternary ammonium and protonated amine cations (cf. Figure 1). The counteranion type and its concentration surrounding the ammonium cations control the strength of electrostatic repulsion (i.e., screening). For chitosan solutions below pH 5, the viscosity and solubility were found to increase as pH decreased, a result attributed to an increase of protonated amine groups.[12−15] At low pH, these studies also showed that the viscosity and solubility increased as counteranion size increases. As the concentration of OH^- increased above pH 6.0, we believe that OH^- replaces some of the Cl^- counteranions surrounding quaternary ammonium and protonated amine cations. A similar ion exchange process was used to generate quaternized copolymer membranes for alkaline fuel cells.[56,57] These studies showed that the replacement of Cl^- counteranions with OH^- resulted in a higher water uptake by the copolymer membranes, which was attributed to the higher affinity of OH^- for water. To better understand the mechanism of swelling, QCM studies of grafted CH-Q will be investigated as a function of quaternary ammonium salt substitution (m in Figure 1), ionic strength, and counteranion type (Y in Figure 1).

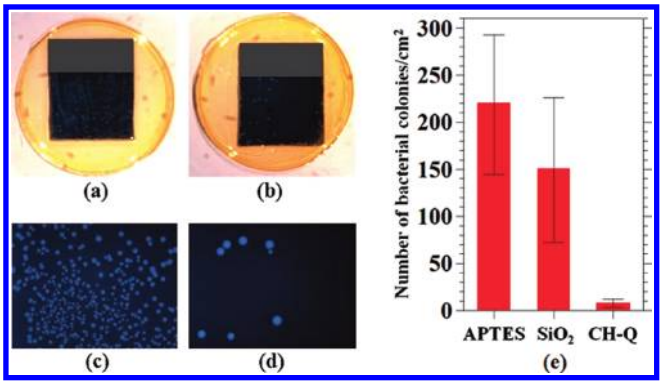

Figure 5. (a) APTES and (b) CH-Q surfaces were immersed in bacterial solution (*S. aureus* in BHI broth, pH 7.3, ~10^4 CFU/mL) at 37 °C for 6 h with shaking (100 rpm). Samples were removed from bacterial solution, immersed in sterilized PBS at 37 °C for 20 min while shaking at 100 rpm, dried in air for 2 min, and incubated under a thin film of TSB agar at 37 °C overnight. Optical photographs (1 cm × 4/3 cm) of bacterial colonies on (c) APTES and (d) CH-Q surfaces. (e) Number of *S. aureus* colonies grown on APTES, SiO_2, and CH-Q surfaces.

Antibacterial Studies. To determine if CH-Q surfaces exhibit antibacterial properties, we performed initial studies to test their resistance to bacterial attachment. Silicon oxide, 3-aminopropyltriethoxysilane (APTES) modified silicon oxide and CH-Q brushes on silicon oxide were incubated with *S. aureus* (ATCC 35556, ~10^4 colony forming units/mL (CFU/mL)) in culture medium for 6 h at pH 7.3. The pH was monitored throughout the experiment and found to remain at 7.3. The number of adherent bacteria, visualized by colony formation under a thin film of TSB agar (Figure 5a−d), decreased on the CH-Q surface, albeit individual colony size was smaller on the APTES surface, possibly due to nutrient deprivation.[58] By direct counting, 219 ± 74, 149 ± 77, and 7 ± 5 colonies/cm^2 of *S. aureus* were present on the APTES, SiO_2, and CH-Q surfaces, respectively (Figure 5e). Whereas no significant differences are observed between the silicon oxide and APTES surfaces, the grafted CH-Q layer exhibits an ~30× reduction in bacterial attachment/growth relative to the APTES surface. Electrostatic interactions alone are unable to account for this behavior because both APTES and CH-Q surfaces are positively charged and *S. aureus* is negatively charged.[39] The antibacterial properties of the CH-Q surface can partly result from the disruption of the bacterial cell membrane due to the quaternary ammonium salts[31−38] tethered to the flexible polymer brush.[59] To better understand the antimicrobial activity of the CH-Q layer, future bacterial adhesion studies will be conducted to investigate the effects of incubation time, to assess numbers of viable versus total bacteria, both on the surface and in solution, and to quantify bacterial adhesion under flow conditions using a parallel plate flow chamber.

IV. CONCLUSIONS

Chitosan modified with quaternary ammonium salts, CH-Q, was grafted to an epoxide-derivatized silicon oxide surface. Using zeta potential measurements, the CH-Q grafted surface displayed a high positive charge between pH 2.97 and 8.21. In situ QCM-D and SE studies yielded consistent results showing that grafted CH-Q is chemically stable over a wide range of pH values and exhibits reversible swelling and contraction that can be tuned by varying the pH of the solution. At pH 5.01, the CH-Q layer

exhibits the least swelling, whereas at higher and lower values of pH the swelling of the CH-Q layer increases up to ~3× relative to the thickness at pH 5.01. The thicknesses and water concentration of the grafted layer measured by SE and QCM-D were in excellent agreement across the pH range. These studies provide new insight about CH-Q layer behavior because, even at pH 5.01 (i.e., minimum layer thickness), the CH-Q layer contains a high concentration of water (78%). Furthermore, relatively small changes in water content (e.g., 78−90%) trigger a large change in the viscoelastic behavior of the CH-Q layer. This pH dependent swelling behavior is of interest for initiating drug release and controlling the channel width of nanofluidic devices as well as other biological applications. To this end, the ability to resist bacterial colonization over a 6 h incubation was tested using *S. aureus*, a common pathogen in deep infection. The grafted CH-Q layer showed significantly reduced bacterial colonization when compared to silicon oxide and APTES modified silicon oxide surfaces. Future antibacterial studies will investigate the function of quaternary ammonium salt concentrations in conferring antibacterial properties for a variety of physiologically relevant Gram-positive and Gram-negative pathogens.

■ ASSOCIATED CONTENT

Supporting Information. Surface thickness and contact angle data, surface zeta potential data, and thickness and shear modulus data. This material is available free of charge via the Internet at http://pubs.acs.org.

■ AUTHOR INFORMATION

Corresponding Author

*Mailing address: Materials Science and Engineering, University of Pennsylvania, Laboratory for Research on the Structure of Matter, 3231 Walnut Street, Philadelphia, Pennsylvania 19104, United States. Telephone: 215 898 4451. E-mail: composto@seas.upenn.edu.

■ ACKNOWLEDGMENT

This work was supported by the National Institutes of Health (NIH R01 HL60230, R.J.C. and D.M.E.). R.J.C. also thanks NSF/NBIC (DMR08-32802) and Colgate-Palmolive for support. D.L. acknowledges support from the NSF in form of a CAREER grant (DMR-1055594). N.J.H. thanks the NIH (AR-051303, HD-061053, and DE-019901) for support.

■ REFERENCES

(1) Senaratne, W.; Andruzzi, L.; Ober, C. K. *Biomacromolecules* **2005**, *6*, 2427–2448.
(2) Halperin, A.; Tirrell, M.; Lodge, T. P. *Adv. Polym. Sci.* **1992**, *100*, 31–71.
(3) Milner, S. T. *Science* **1991**, *251*, 905–914.
(4) Zhao, B; Brittain, W. J. *Prog. Polym. Sci.* **2000**, *25*, 677–710.
(5) Advincula, R. C.; Brittain, W. J.; Caster, K. C.; Rühe, J. In *Polymer Brushes: Synthesis, Characterization, Applications*; Advincula, R. C., Brittain, W. J., Caster, K. C., Rühe, J., Eds.; Wiley: Weinheim, Germany, 2004.
(6) Ravi Kumar, M. N. V.; Muzzarelli, R. A. A.; Muzzarelli, C.; Sashiwa, H.; Domb, A. J. *Chem. Rev.* **2004**, *104*, 6017–6084.
(7) Rinaudo, M. *Prog. Polym. Sci.* **2006**, *31*, 603–632.
(8) Kim, I.; Seo, S.; Moon, H.; Yoo, M.; Park, I.; Kim, B.; Cho, C. *Biotechnol. Adv.* **2008**, *26*, 1–21.
(9) Rabea, E. I.; Badawy, M. E.-T.; Stevens, C. V.; Smagghe, G.; Steurbaut, W. *Biomacromolecules* **2003**, *4*, 1457–1465.
(10) Yi, H.; Wu, L.; Bentley, W. E.; Ghodssi, R.; Rubloff, G. W.; Culver, J. N.; Payne, G. F. *Biomacromolecules* **2005**, *6*, 2881–2894.
(11) Payne, G. F.; Raghavan, S. R. *Soft Matter* **2007**, *3*, 521–527.
(12) Hamdine, M.; Heuzey, M.; Begin, A. *Int. J. Biol. Macromol.* **2005**, *37*, 134–142.
(13) Chen, R. H.; Lin, W. C.; Lin, J. H. *Acta Polym.* **1994**, *45*, 41–46.
(14) Sakiyama, T.; Chu, C.; Fujii, T.; Yano, T. *J. Appl. Polym. Sci.* **1993**, *50*, 2021–2025.
(15) Pack, J. W.; Choi, K.; Pack, K. K. *Bull. Korean Chem. Soc.* **1983**, *4*, 68–72.
(16) Sashiwa, H.; Yamamori, N.; Ichinose, Y.; Sunamoto, J.; Aiba, S. *Biomacromolecules* **2003**, *4*, 1250–1254.
(17) Huh, M. W.; Kang, I.; Lee, D. H; Kim, W. S.; Lee, D. H.; Park, L. S.; Min, K. E.; Seo, K. H. *J. Appl. Polym. Sci.* **2001**, *81*, 2769–2778.
(18) Stuart, M. A. C.; Huck, W. T. S.; Genzer, J.; Müller, M.; Ober, C.; Stamm, M.; Sukhorukov, G. B.; Szleifer, I.; Tsukruk, V. V.; Urban, M.; Winnik, F.; Zauscher, S.; Luzinov, I.; Minko, S. *Nat. Mater.* **2010**, *9*, 101–113.
(19) Abu-Lail, N. I.; Kaholek, M.; LaMattina, B.; Clark, R. L.; Zauscher, S. *Sens. Actuators, B* **2006**, *114*, 371–378.
(20) Lee, H.; Penn, L. S. *Macromolecules* **2008**, *41*, 8124–8129.
(21) Ayres, N.; Boyes, S. G.; Brittain, W. J. *Langmuir* **2007**, *23*, 182–189.
(22) Wu, T.; Gong, P.; Szleifer, I.; Vlcek, P.; Subr, V.; Genzer, J. *Macromolecules* **2007**, *40*, 8756–8764.
(23) Jhon, Y. K.; Bhat, R. R.; Jeong, C.; Rojas, O. J.; Szleifer, I.; Genzer, J. *Macromol. Rapid Commun.* **2006**, *27*, 697–701.
(24) Moya, S.; Azzaroni, O.; Farhan, T.; Osborne, V. L.; Huck, W. T. S. *Angew. Chem., Int. Ed.* **2005**, *44*, 4578–4581.
(25) Xu, C.; Wu, T.; Drain, C. M.; Batteas, J. D.; Fasolka, M. J.; Beers, K. L. *Macromolecules* **2006**, *39*, 3359–3364.
(26) Draper, J.; Luzinov, I.; Minko, S.; Tokarev, I.; Stamm, M. *Langmuir* **2004**, *20*, 4064–4075.
(27) Hiller, J.; Rubner, M. F. *Macromolecules* **2003**, *36*, 4078–4083.
(28) Itano, K.; Choi, J.; Rubner, M. F. *Macromolecules* **2005**, *38*, 3450–3460.
(29) Zasloff, M. *Nature* **2002**, *415*, 389–395.
(30) Bromberg, L.; Hatton, T. A. *Polymer* **2007**, *48*, 7490–7498.
(31) Kenawy, E.; Worley, S. D.; Broughton, R. *Biomacromolecules* **2007**, *8*, 1359–1384.
(32) Lewis, K.; Klibanov, A. M. *Trends Biotechnol.* **2005**, *23*, 343–348.
(33) Lichter, J. A.; Van Vlient, K. J.; Rubner, M. F. *Macromolecules* **2009**, *42*, 8573–8586.
(34) Li, Z.; Lee, D.; Sheng, X.; Cohen, R. E.; Rubner, M. F. *Langmuir* **2006**, *22*, 9820–9823.
(35) Lee, S. B.; Koepsel, R. R.; Morley, S. W.; Matyjaszewski, K.; Sun, Y.; Russell, A. J. *Biomacromolecules* **2004**, *5*, 877–882.
(36) Kurt, P.; Wood, L.; Ohman, D. E.; Wynne, K. J. *Langmuir* **2007**, *23*, 4719–4723.
(37) Yuan, S. J.; Pehkonen, S. O.; Ting, Y. P.; Neoh, K. G.; Kang, E. T. *Langmuir* **2010**, *26*, 6728–6736.
(38) Tiller, J. C.; Liao, C.; Lewis, K.; Klibanov, A. M. *Proc. Natl. Acad. Sci. U.S.A.* **2001**, *98*, 5981–5985.
(39) Ouhara, K.; Komatsuzawa, H.; Kawai, T.; Nishi, H.; Fujiwara, T.; Fujiue, Y.; Kuwabara, M.; Sayama, K.; Hashimoto, K.; Sugai, M. *J. Antimicrob. Chemother.* **2008**, *61*, 1266–1269.
(40) Sauerbrey, G. *Z. Phys.* **1959**, *155*, 206–222.
(41) Vogt, B. D.; Lin, E. K.; Wu, W.; White, C. C. *J. Phys. Chem. B* **2004**, *108*, 12685–12690.
(42) Hook, F.; Kasemo, B.; Nylander, T.; Fant, C.; Sott, K.; Elwing, H. *Anal. Chem.* **2001**, *73*, 5796–5804.
(43) Brunner, H.; Vallant, T.; Mayer, U.; Haffmann, H. *J. Colloid Interface Sci.* **1999**, *212*, 545–552.
(44) Hiller, J.; Mendelsohn, J. D.; Rubner, M. F. *Nat. Mater.* **2002**, *1*, 59–63.
(45) Lee, M. H.; Brass, D. A.; Morris, R.; Composto, R. J.; Ducheyne, P. *Biomaterials* **2005**, *26*, 1721–1730.

(46) Lee, M. H.; Boettiger, D.; Ducheyne, P.; Composto, R. J. In *Silanes and Other Coupling Agents*; Mittal, K. L., Ed.; VSP: Brill, Leiden, 2007; Vol. 4, pp 1−16.
(47) Adamczyk, Z.; Zaucha, M.; Zembala, M. *Langmuir* **2010**, *26*, 9368–9377.
(48) Walker, S. L.; Bhattacharjee, S.; Hoek, E. M. V.; Elimelech, M. *Langmuir* **2002**, *18*, 2193–2198.
(49) Scales, P. J.; Grieser, F.; Healy, T. W.; White, L. R.; Chan, D. Y. C. *Langmuir* **1992**, *8*, 965–974.
(50) Gong, P.; Wu, T.; Genzer, J.; Szleifer, I. *Macromolecules* **2007**, *40*, 8765–8773.
(51) Aklonis, J. J.; Knight, W. J. *Introduction to Polymer Viscoelasticity*, 2nd ed.; John Wiley & Sons: New York, 1983; Chapter 7.
(52) Anthonsen, M. W.; Varum, K. M.; Smidstrod, O. *Carbohydr. Polym.* **1993**, *22*, 193–201.
(53) Cho, J.; Heuzey, M.; Begin, A.; Carreau, P. J. *J. Food Eng.* **2006**, *74*, 500–515.
(54) Jiang, H.; Su, W.; Caracci, S.; Bunning, T. J.; Cooper, T.; Adams, W. W. *J. Appl. Polym. Sci.* **1996**, *61*, 1163–1171.
(55) Solimini, D. *J. Appl. Phys.* **1966**, *37*, 3314–3315.
(56) Zhang, Q; Zhang, Q; Wang, J; Zhang, S; Li, S. *Polymer* **2010**, *51*, 5407–5416.
(57) Xu, H.; Fang, J; Guo, M; Lu, X; Wei, X.; Tu, S. *J. Membr. Sci.* **2010**, *354*, 206–211.
(58) Lichter, J. A.; Thompson, M. T.; Delgadillo, M.; Nishikawa, T.; Rubner, M. F.; Van Vlient, K. J. *Biomacromolecules* **2008**, *9*, 1571–1578.
(59) Lichter, J. A.; Rubner, M. F. *Langmuir* **2009**, *25*, 7686–7694.